SPATIAL CORRELATION OF PUTATIVE WATER RELATED FEATURES IN CYDONIA MENSAE AND SOUTHERN ACIDALIA PLANITIA. E. M. McGowan[1] and G. E. McGill[2], [1,2]Department of Geosciences, University of Massachusetts, Amherst, MA 01003. emcgowan@geo.umass.edu and gmcgill@geo.umass.edu.

Introduction: To understand the distribution and timing of water on Mars we are mapping and spatially analyzing the putative water-related features in the northern lowland of Mars. Earlier we examined [1] the distribution of rampart craters vs. all other craters in Utopia Planitia and found that their distribution differed. This study addresses the spatial distribution of pitted cones and the relationship of this distribution to putative shorelines located in the Cydonia Mensae-Southern Acidalia Planitia area [2], which we will call the study area. This area is bounded by 340°-355°E and 37.5°-47.5°N. and includes part of the dichotomy boundary that is gradational [3] and characterized by clusters of knobs and mesas. We use a Geographic Information System (GIS) to help visualize and measure the clustering and density of pitted cones and their proximity to inferred shorelines [3, 4, 5].

Pitted cones: Small cones (diameter 800m) were first seen in Viking imagery [6]. These small cone-like features, most with summit pits, are abundant in the northern lowlands. Various origins have been suggested, all of which, except for cinder cones, are related to water or ice.

1. mud volcanoes [7, 8, 9, 10]
2. pingos [11]
3. cinder cones [12]
4. rootless cones (pseudo-craters) [6, 13, 14, 15, 16, 17, 18]

A study of pitted cone morphology in the Acidalia/Cydonia region [9] found morphological differences based on latitude. The northern pitted cones located in Acidalia Planitia (centered at 44°N, 21°W) are larger and dome shaped and have slightly higher thermal inertia then the southern cones. The southern cones located in Cydonia Mensae (centered at 34°N, 9°W and extending from Acidalia on the west to 0° longitude and from approximately 30°N to 40°N latitude) are smaller and cone-shaped. The boundary between the northern and southern areas is at ~40.5°N. Parts of both are in our study area.

Shorelines: Putative shorelines were first identified by Parker et al. [3, 4] from Viking image data. Since the availability of Mars Orbiter Laser Altimeter (MOLA) topography, the validity of these features as shorelines has been tested by determining if they are equipotential. Most of these tests have been inconclusive and the existence of putative shorelines is hotly debated [19, 20, 21, 22, 23, 24]

However, Webb [5], using more robust methods, showed that some putative shorelines are at least locally equipotential. In the Cydonia/Acidalia area Webb [5] found two sections of the Deutorenilus shoreline to be equipotential with elevations of -4200m (contact A) and –4000m (contact B). Contact A is contained within our study area.

Methods: The distribution of the pitted cones was taken directly from a published geological map [2]. The pitted cone population consists of all cones with resolvable pits in the high resolution (~42m/px) Viking images used to construct the map. This is the highest resolution continuous data set available for the study area. The map was georeferenced in a GIS and the pitted cones were digitized. We used Mars Orbiter Camera (MOC) narrow-angle images and Thermal Emission Imaging System visible images (Themis VIS) to examine pitted cone morphology. Webb's [5] Contact A was also georeferenced to our data set. The base for georeferencing is a 231m/px topographic model created in the GIS that is used to correlate elevation with features (fig. 1).

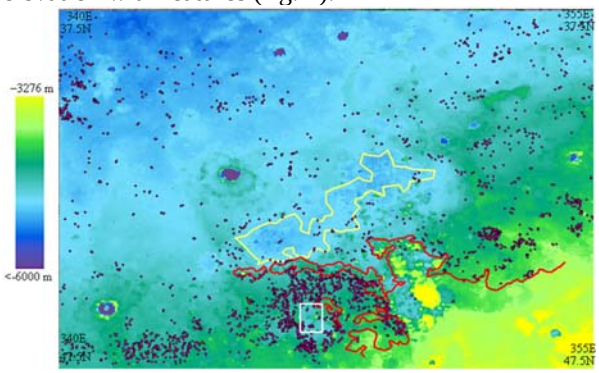

Figure 1 Topographic map of the study area. Pitted cones are dark red, Contact A (putative shoreline) is red, yellow encloses an area of polygonal terrain, and the white box indicates location of figure 3.

Using the GIS we ran a density function module that defines a neighborhood as a circle with a pitted cone in the middle. Other pitted cones in the neighborhood (within the circle) are counted and that number is divided by the area of the neighborhood (circle). This is repeated for each pitted cone throughout the study area. The result is a map showing the density distribution of pitted cones within the study area (fig. 2).

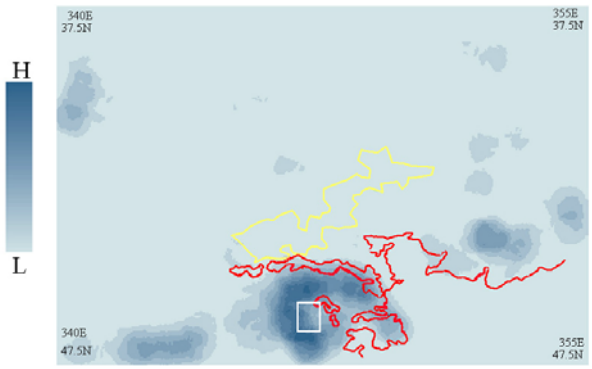

Figure 2: Results of density analysis of mapped pitted cones in the study area. This image shows the relationship between areas of high density (dark blue) and Contact A (putative shoreline) shown in red. Area inside yellow boundary has very well defined polygonal terrain and has a low density of pitted cones. White box indicates location of figure 3.

Observations: While pitted cones are distributed throughout most of the study area, several distinct clusters are obvious (fig. 2). Although small clusters are evident in the northern section of the study area 70% are located in the southern third. The most pronounced cluster is in close proximity to and just south of contact A [5] (fig. 2). This large cluster surrounds a local low area containing an elongated knob from which linear troughs radiate (fig. 3). These troughs are similar to ones that characterize giant polygons. Pitted cones are rare within this local low area. North of Contact A pitted cones roughly surround an ovoidal low area that is characterized by polygonal terrain and a paucity of pitted cones (fig. 2).

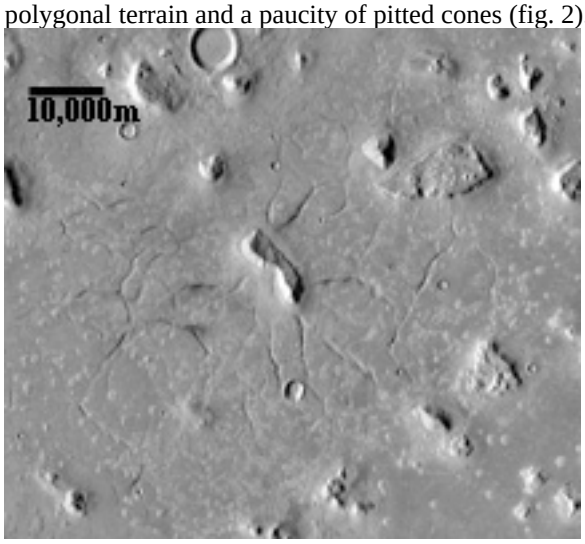

Figure 3: Low area indicated in figures 1 and 2 by white box. Oblong knob surrounded by radial fractures resembling polygonal terrain. Area contains few pitted cones. Mosaic of Viking images 72a01,72a02, 72a03, 72a04.

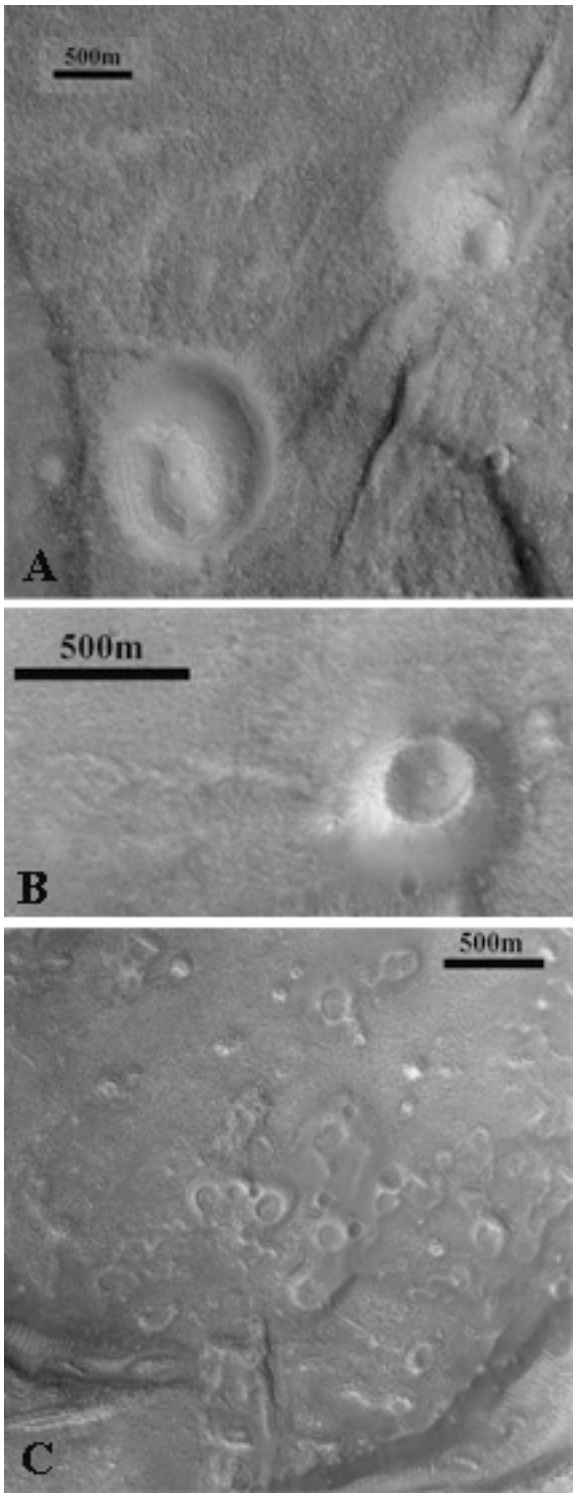

Figure 4: Examples of three different morphologies of pitted cones present in the study area. A) MOC narrow angle image m0400576 centered at 42.27°N-11.10°W showing pitted domes, B) MOC narrow angle image mm0304566 centered at 40.73°N-9.89°W showing pitted cone, C) MOC narrow angle image m0705393 centered at 38.59°N-12.92°W ring structures.

Based on widely scattered MOC and THEMIS VIS images it is possible to define several morphologies of pitted cones in the study area
(fig. 4). The most abundant are simple cone-shaped constructs with summit pits that are small relative to the diameter of the cones. Other structures are dome like. In the southern area are fields of small craters that have pits that encompass all but an outside wall, forming a ring-like morphology. These structures closely resemble Icelandic pseudo-craters (6, 13, 14, 15). Most are below the resolution of the Viking Images. Owing to the spotty coverage by MOC and THEMIS VIS images we have not been able to determine any spatial correlations among the various types of pitted cones.

The elevation range for the study area is -3276m to –4900m a range of 1624m (ignoring the deepest crater floors). Almost all (92%) pitted cones identified by McGill in 2005 on Viking images occur at elevations between -4674 and –4130, a range of 544m (fig. 5).

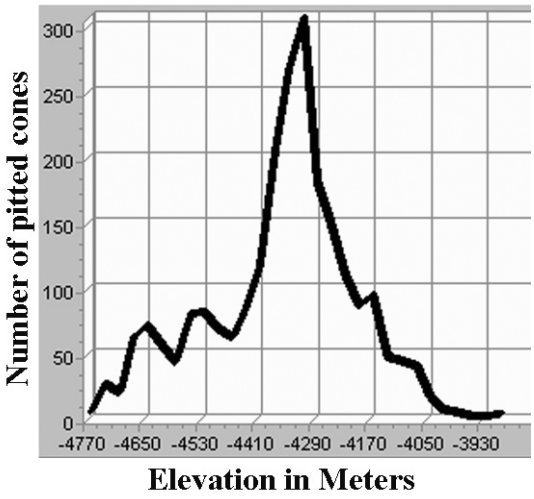

Figure 5: Histogram showing relationship between pitted cones and elevation

Discussion: In the Cydonia Mensae area there is a qualitative spatial correlation between the putative Deuteronilus shoreline (Contact A [3, 4, 5]) and pitted cone occurrence. The greatest clustering of pitted cones occurs in what would have been a semi-enclosed bay, assuming that contact A is a paleo-shoreline. In addition the occurrence of pitted cones, although at low elevations, diminishes with the lowest elevations. Owing to the proximity of the large numbers of pitted cones and putative shorelines in the Cydonia area we plan to investigate possible shoreline and backshore processes that would contribute to the formation of the various types of pitted cones observed in the study area.

References: [1] McGowan, E. M. and McGill, G. E. (2007) *LPSC XXXVII* Abstract #1022. [2] McGill, G. E. (2005), USGS Map, *Geologic Investigation Series I-2811*. [3]Parker, T. J. *et al.* (1989) *Icarus, 82*, 111–145. [4] Parker, T. J. *et al.* (1993) *JGR, 98*, 11061-11078. [5] Webb, V. E. (2004) *JGR, 109*, E09010, doi:10.1029/2003JE002205. [6] Frey, H. *et al.* (1979) *JGR*, 84, 8075-8086. [7] Tanaka, K. L. (1997) *JGR, 102*, 4131-4149. [8] Tanaka, K. L. *et al.* (2003) *JGR, 108*(E4), 8043, doi: 10.1029/2002JE001908. [9] Farrand, W. H. *et al.* (2005) JGR, 110, E05005, doi:10.1029/2004JE002297. [10] Skinner, J. A. and Tanaka, K. L. (2007) *Icarus, 186*, 41-59. [11] Lucchitta, B. K. (1981) *Icarus*, 45, 264-303. [12] Wood, C. A. (1979) *LPSC X*, 2815-2840. [13] Frey, H. and Jarosewich, M. (1982) *JGR, 87*, 9867-9879. [14] Greeley R. and Fagents, S. A. (2001) *JGR, 106*, 20527–20546. [15] Lanagan, P. D. *et al.* (2001) *GRL, 28*, 2365-2367. [16] Bruno, B. C. *et al.* (2004) *JGR, 109*, E07009, doi:10.1029/2004JE002273. [17] Bruno, B. C. *et al.* (2006) *JGR, 111*, E06017, doi:10.1029/2005JE002510. [18] Baloga, S. M. et al. (2007) *JGR, 112*, E03002, doe:10.1029/2005JE002652. [19] Head III, J. W. *et al.* (1998) *GRL, 25*(24), 4401-4404. [20] Heisinger, H. and Head III, J. W. (2000) *JGR, 105* (E5), 11,999-12,022. [21] Carr, M. H. and Head III, J. W. (2003) *JGR,108*, No. E5, 5042, doi:1029/2002JE001963. [22] Heisinger *et al.*, (2000) *LPSC, XXXI*, abs. #1646. [23] Leverington, D. W. and Ghent, R. R. (2004) *JGR* **109**, E01005,10.1029/2003JE002141.
[24] Malin, M. C. and Edgett, K. S. (1999) *Jour. Geophys. Res.*, 106(E10), 23429–23570, doi: 10.1029/2000JE001455.